Basics of plasma spectroscopy

Basics of plasma spectroscopy

U Fantz

Max-Planck-Institut für Plasmaphysik, EURATOM Association Boltzmannstr. 2, D-85748
Garching, Germany

E-mail: fantz@ipp.mpg.de

Abstract
These lecture notes are intended to give an introductory course on plasma
spectroscopy. Focusing on emission spectroscopy, the underlying principles
of atomic and molecular spectroscopy in low temperature plasmas are
explained. This includes choice of the proper equipment and the calibration
procedure. Based on population models, the evaluation of spectra and their
information content is described. Several common diagnostic methods are
presented, ready for direct application by the reader, to obtain a multitude of
plasma parameters by plasma spectroscopy.

1. Introduction

Plasma spectroscopy is one of the most established and
oldest diagnostic tools in astrophysics and plasma physics
(see for example [1, 2]). Radiating atoms, molecules and
their ions provide an insight into plasma processes and plasma
parameters and offer the possibility of real-time observation.
Emission spectra in the visible spectral range are easy to
obtain with a quite simple and robust experimental set-up.
The method itself is non-invasive, which means that the
plasma is not affected. In addition, the presence of rf fields,
magnetic fields, high potentials etc. does not disturb the
recording of spectra. Also the set-up at the experiment
is very simple: only diagnostic ports are necessary which
provide a line-of-sight through the plasma. Thus plasma
spectroscopy is an indispensable diagnostic technique in
plasma processing and technology as well as in fundamental
research. Although spectra are easily obtained, interpretation
can be fairly complex, in particular, in low temperature, low
pressure plasmas which are far from thermal equilibrium, i.e.
non-equilibrium plasmas.

These notes give an introduction to plasma spectroscopy
of low temperature plasmas for beginners. For further
reading the following selection of books is recommended.
Principles and fundamental techniques of plasma spectroscopy
are very well described in [3, 4]. Elementary processes that
determine the radiation of atoms and molecules in plasmas
are discussed in detail in [5]. An introduction to low
temperature plasma physics and common diagnostic methods
with focus on applications to plasma processing is given in
[6, 7]. An overview of plasma diagnostic methods for various
applications can be found in [8–10]. Applications of plasma
spectroscopy for purposes of chemical analysis are described
in [11–14].

2. Radiation in the visible spectral range

Electromagnetic waves extend over a wide wavelength range,
from radio waves (kilometre) down to γ-rays (picometer). The
visible range is only a very small part ranging from 380 to
780 nm by definition. However, common extensions are to the
ultraviolet and the infrared resulting roughly in a range from
200 nm to 1 μm. From the experimental point of view this
wavelength region is the first choice in plasma spectroscopy:
air is transparent, quartz windows can be used and a variety of
detectors and light sources are available. Below 200 nm quartz
glass is no longer transparent and the oxygen in the air starts to
absorb light resulting in the requirement of an evacuated light
path. Above 1 μm the thermal background noise becomes
stronger which can only be compensated for by the use of
expensive detection equipment.

Radiation in the visible spectral range originates from
atomic and molecular electronic transitions. Thus, the heavy
particles of low temperature plasmas, the neutrals and their
ions basically characterize the colour of a plasma: typically a
helium plasma is pink, neon plasmas are red, nitrogen plasmas
are orange and hydrogen are purple—these are first results of
spectroscopic diagnostics using the human eye.

2.1. Emission and absorption

In general, plasma spectroscopy is subdivided into two types of
measurements: the passive method of emission spectroscopy
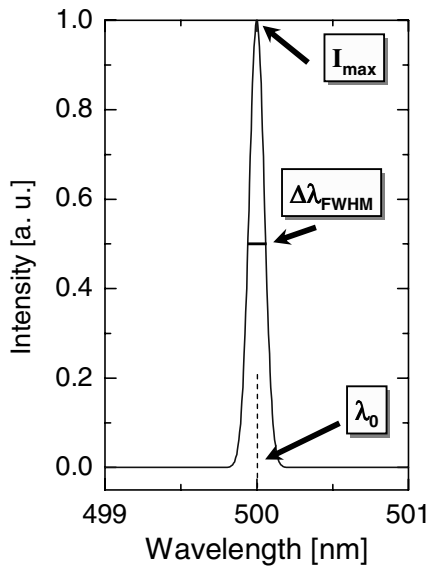and the active method of absorption spectroscopy. In the case

Figure 1. Line radiation and its characteristics.

of emission spectroscopy, light emitted from the plasma itself is recorded. Here, one of the basic underlying processes is the excitation of particles (atoms, molecules, ions) by electron impact from level q to level p and the decay into level k by spontaneous emission with the transition probability A_{pk} resulting in line emission ε_{pk}. In the case of absorption spectroscopy, the excitation from level q to level p takes place by a radiation field (i.e. by absorption with the transition probability B_{qp}) resulting in a weakening of the applied radiation field which is recorded. The intensity of emission is correlated with the particle density in the excited state $n(p)$, whereas the absorption signal correlates with the particle density in the lower state $n(q)$, which is in most cases the ground state. Thus, ground state particle densities are directly accessible by absorption spectroscopy; however, absorption techniques need much more experimental effort than emission spectroscopy. Since some principles of emission spectroscopy apply also to absorption and, since emission spectroscopy provides a variety of plasma parameters and is a passive and very convenient diagnostic tool these lecture notes are focused on emission spectroscopy. Further information on absorption techniques and analysis methods can be found in [6, 7, 15, 16].

The two axes of a spectrum are the wavelength axis and the intensity axis as shown in figure 1. The central wavelength of line emission λ_0 is given by the photon energy $E = E_p - E_k$ corresponding to the energy gap of the transition from level p with energy E_p to the energetically lower level k (Planck constant h, speed of light c):

$$\lambda_0 = h\,c/(E_p - E_k)\,. \tag{1}$$

Since the energy of a transition is a characteristic of the particle species, the central wavelength is an identifier for the radiating particle, unless the wavelength is shifted by the Doppler effect. As a principle, the wavelength axis λ is easy to measure, to calibrate and to analyse. This changes to the opposite for the intensity axis. The line intensity is quantified by the line emission coefficient:

$$\varepsilon_{pk} = n(p)\,A_{pk}\frac{h\,c}{4\pi\,\lambda_0} = \int_{\text{line}} \varepsilon_\lambda\,\mathrm{d}\lambda \tag{2}$$

in units of $W\,(m^2\,sr)^{-1}$, where 4π represents the solid angle $d\Omega$ (isotropic radiation), measured in steradian (sr). The line profile P_λ correlates the line emission coefficient with the spectral line emission coefficient ε_λ:

$$\varepsilon_\lambda = \varepsilon_{pk} P_\lambda \quad\text{with}\quad \int_{\text{line}} P_\lambda\,\mathrm{d}\lambda = 1\,. \tag{3}$$

A characteristic of the line profile is the full width at half maximum (FWHM) of the intensity, $\Delta\lambda_{\text{FWHM}}$, as indicated in figure 1. The line profile depends on the broadening mechanisms [4]. In the case of Doppler broadening the profile is a Gaussian profile; the line width correlates with the particle temperature (see section 4.2). A convenient alternative to the line emission coefficient (equation (2)) is the absolute line intensity in units of photons $(m^3\,s)^{-1}$:

$$I_{pk} = n(p)A_{pk}\,. \tag{4}$$

This relationship reveals that the line intensity depends only on the population density of the excited level $n(p)$ which, in turn, depends strongly on the plasma parameters $n(p) = f(T_e, n_e, T_n, n_n, ...)$. This dependence is described by population models and will be discussed in section 3.

2.2. Atomic and molecular spectra

The atomic structure of atoms and molecules is commonly represented in an energy level diagram and is strongly related to emission (and absorption) spectra. The electronic energy levels of atoms and diatomic molecules have their spectroscopic notation:

$$n\ell^{\text{w}\ 2S+1}L_{L+S} \qquad\text{and}\qquad n\ell^{\text{w}\ 2S+1}\Lambda_{\Lambda+\Sigma}{}^{+,-}_{g,u}\,, \tag{5}$$

respectively. n is the main quantum number, ℓ the angular momentum, w the number of electrons in the shell, S the spin, $2S+1$ the multiplicity, $L+S = J$ the total angular momentum. This represents the LS coupling which is valid for light atoms. Details of atomic structure can be found in the standard books, e.g. [17–20]. In case of diatomic molecules the projection of the corresponding vectors onto the molecular axis is important, indicated by Greek letters. $+, -$ and g, u denote the symmetry of the electronic wave function (for details see [4,20–22]). Optically allowed transitions follow the selection rules for dipole transitions which can be summarized as: $\Delta L = 0, \pm 1$, $\Delta J = 0, \pm 1$, $\Delta S = 0$ for atoms and $\Delta\Sigma = 0$, $u \leftrightarrow g$ for molecules. $\Delta L = 0$ or $\Delta J = 0$ transitions are not allowed if the angular momenta of both states involved are zero.

Figure 2 shows the energy level diagram for helium which is a two electron system. The levels are separated into two multiplet systems: a singlet and a triplet system. Following Pauli's principle the spin of two electrons in the ground state is arranged anti-parallel resulting in the $1s\ 1^1S$ state. The fine structure is indicated only for the 2^3P state. Electronic states which cannot decay via radiative transitions have a long lifetime and are called metastable states (2^3S and 2^1S). Transitions which are linked directly to the ground state are called resonant transitions. The corresponding transition probability is high, hence the radiation is very intense. Due to the large energy gap these transitions are often in the vacuum ultraviolet (vuv) wavelength range. Optically allowed
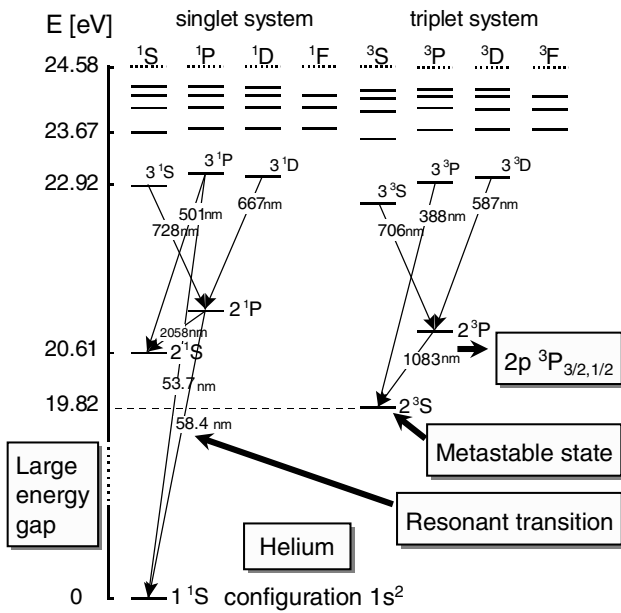
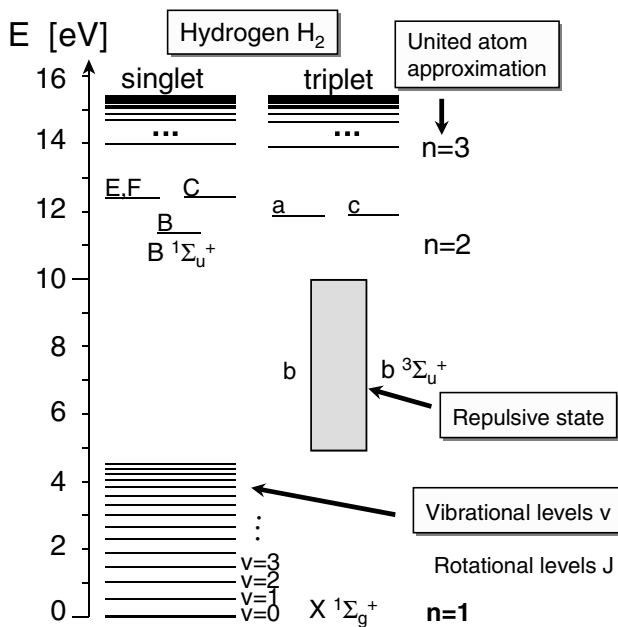**Figure 2.** Example of an atomic energy level diagram.

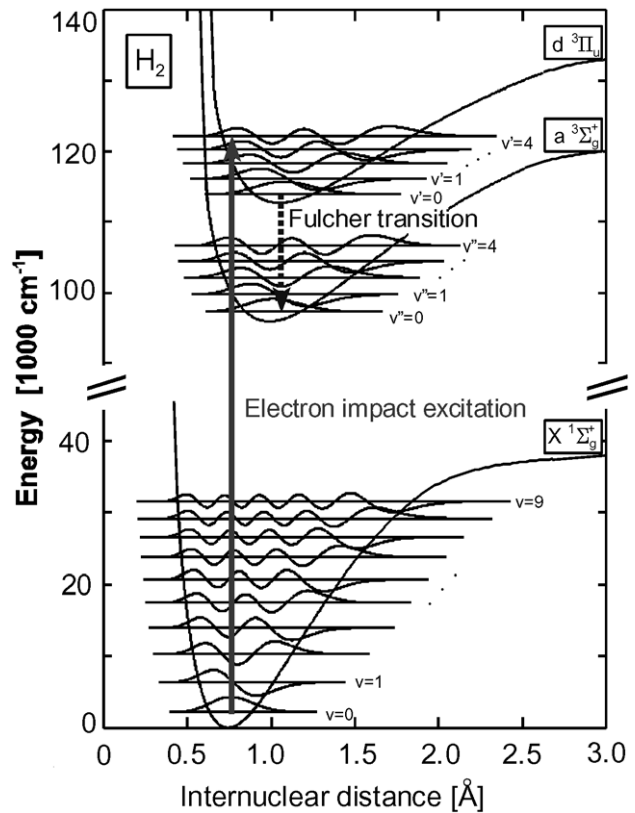**Figure 3.** Example of an energy level diagram of a diatomic molecule.

Figure 4. Molecular excitation and radiation according to the Franck–Condon principle for the ground state and two excited states of molecular hydrogen.

transitions with upper quantum number $n \leqslant 3$ are indicated by an arrow and labelled with the corresponding wavelength. Radiation in the visible spectral range mostly originates from transitions between excited states.

The energy level diagram of a diatomic molecule with two electrons, i.e. molecular hydrogen, is shown schematically in figure 3. Again the two electrons cause a splitting into a singlet and a triplet system. In the united atom approximation for molecules a main quantum number can be assigned. In molecules the energy levels are usually abbreviated by upper and lower case letters, where X is the ground state (as a rule). The corresponding spectroscopic notation is shown in figure 3 for the X and b states. Due to the additional

degrees of freedom, each electronic state has vibrational levels (quantum number v) and each vibrational level has rotational levels (quantum number J) which appear with decreasing energy distances. The vibrational levels in the ground state are indicated in figure 3. A special feature in the energy level diagram of the hydrogen molecule is the repulsive state $b\,^3\Sigma_u^+$. Due to the repulsive potential curve, the energy range covers a few electronvolts. Molecules in this state eventually dissociate. Radiation in the visible spectral range correspond to an electronic transition without restrictions for the change in the vibrational quantum number and appear in the spectrum as vibrational bands. Each vibrational band has a rotational structure, where the rotational lines must follow the selection rules: $\Delta J = 0, \pm 1$, forming so-called $P-$, $Q-$ and $R-$branches.

An additional feature of diatomic molecules is the internuclear distance of the two nuclei. Thus, potential curves define the energy levels. This is shown in figure 4 for the ground state and two electronically excited states of hydrogen together with vibrational levels, i.e. the vibrational eigenvalues and the corresponding vibrational wave functions. Under the assumption that the internuclear distance does not change in the electron impact excitation process and during the decay by spontaneous emission, excitation and de-excitation follow a vertical line in figure 4, which means that the Franck–Condon principle is valid. In other words, a vibrational population in the ground state is projected via the Franck–Condon factors into the electronically excited state. The Franck–Condon factor is defined as the overlap integral of
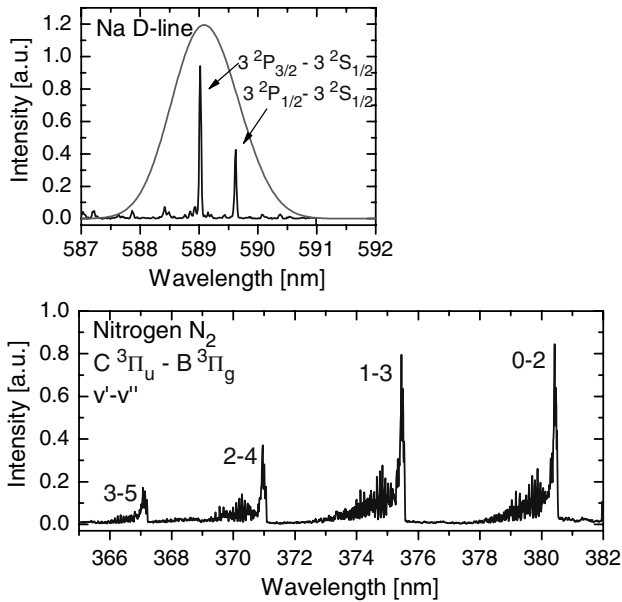
Figure 5. Atomic and molecular spectra: NaD-lines and vibrational bands of the second positive system of N_2.

two vibrational wave functions. In addition for radiative transitions the electronic dipole transition momentum has to be taken into account. Thus, the Franck–Condon factors are replaced by vibrational transition probabilities and together with the vibrational population of the excited state determine the intensity of a vibrational band.

Figure 5 shows the intense vibrational bands of molecular nitrogen. These vibrational bands $v' - v''$ with $\Delta v = 2$ (v' is the vibrational quantum number in the upper electronic state, v'' is the vibrational quantum number in the lower electronic state) correspond to the electronic transition $C\,^3\Pi_u$–$B\,^3\Pi_g$, which is called the second positive system of nitrogen. The rotational structure of each vibrational band is observed clearly: however, the shape of the bands is determined by the spectral resolution of the spectroscopic system. The same applies to atomic spectra as shown in the upper part of figure 5 for sodium. The two narrow lines correspond to a recorded spectrum where the fine structure is resolved, whereas the broad line would be observed by a spectrometer with poor spectral resolution, a quantity which will be discussed in the next section.

2.3. Spectroscopic systems

The choice of spectrographs, detectors and optics depends strongly on the purpose for which the diagnostic tool is to be used. Details of various spectroscopic systems and their components can be looked up in standard books about optics or in [3,4]. The basic components of a spectrometer are: the entrance and exit slit, the grating as the dispersive element and the imaging mirrors, as illustrated in figure 6 for the Czerny–Turner configuration. The exit slit is equipped with a detector. The light source, i.e. the plasma, is either imaged by an imaging optics onto the entrance slit or coupled by fibres to the slit. The latter is very convenient, particularly when direct access to the plasma light is difficult. The individual parts of
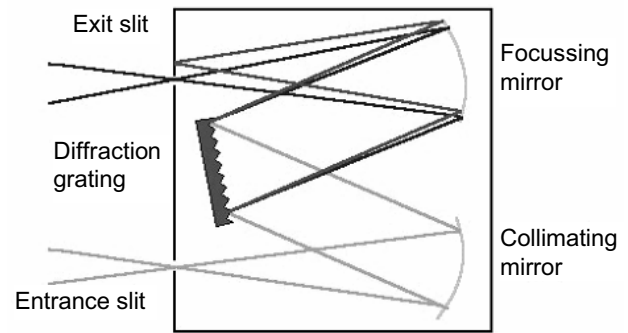

Figure 6. Monochromator in Czerny–Turner configuration.

the spectroscopic system determine the accessible wavelength range, the spectral resolution and the throughput of light.

The choice of the grating, which is characterized by the grooves per millimetre (lines/mm) is of importance for the spectral resolution. Special types of gratings such as Echelle gratings are optimized for high order diffractions resulting in a high spectral resolution. The blaze angle of a grating determines the wavelength range with highest reflection efficiency, i.e. the sensitivity of the grating.

The focal length of the spectrometer influences the spectral resolution and together with the size of the grating defines the aperture and thus the throughput of light. The width of the entrance slit is also of importance for light throughput, which means a larger entrance slit results in more intensity, with the drawback that the spectral resolution decreases.

At the exit either a photomultiplier is mounted behind the exit slit or a CCD (charge-coupled device) array is mounted directly at the image plane of the exit. In the first case, the width of the exit slit or, in the second case, the pixel size influence the spectral resolution of the system. The overall sensitivity of the system is strongly dominated by the type of detector: photomultipliers with different cathode coatings or CCD arrays with different sensor types (intensified, back-illuminated, etc.). Spectroscopic systems which use photomultipliers are scanning systems whereas systems with CCD arrays are capable of recording a specific wavelength range. Spatial resolution can be achieved by the choice of 2-dim detectors. Temporal resolution is completely determined by the detector: photomultipliers are usually very fast, whereas CCD arrays are limited by the exposure time and read-out time.

In the following some typical system set-ups are presented in order to give an overview of the different types of spectrometers and their typical application. For line monitoring, which means following the temporal behaviour of an emission line, pocket size survey spectrometers are very suitable. They have a poor spectral resolution $\Delta\lambda \approx 1$–2 nm but a good time resolution. The diagnostic technique itself is a simple one, providing information on plasma stability or changes in particle densities. Another typical system is a spectrometer with a focal length of 0.5–1 m ($\Delta\lambda \approx 40$ pm) and a grating with 1200 lines mm^{-1}. The optical components and the optics are very much improved; the time resolution depends on the detector. Using a 2–dim CCD camera reasonable spatial resolution can be achieved. This combination represents a flexible system and is a reasonable compromise between spectral resolution and temporal behaviour.

The next step is to deploy an Echelle spectrometer, which provides an excellent spectral resolution ($\Delta\lambda \approx 1$–2 pm) by making use of the high orders of diffraction provided by the special Echelle grating. Typical applications are measurements of line profiles and line shifts. An important point in the choice of the spectroscopic system is the intensity of the light source. For example, measurements with an Echelle spectrometer require much more light than measurements with the survey spectrometer. However, this can be partly compensated by the choice of detector and exposure time.

Another important issue is the calibration of the spectroscopic system. One part is the calibration of the wavelength axis, which is an easy task, done by using spectral lamps (or the plasma itself) in combination with wavelength tables [23]. For example a mercury–cadmium lamp can be used as the cadmium and mercury lines extend over a wide wavelength range. Groups of lines with various distances between each other (wavelength axis) are very well suited to determine the spectral resolution of the system and the apparatus profile. In this case, line broadening mechanisms must be excluded, for example, by using low pressure lamps.

Much more effort is needed for the calibration of the intensity axis, which can be either a relative or an absolute calibration. A relative calibration takes into account only the spectral sensitivity of the spectroscopic system along the wavelength axis. An absolute calibration provides in addition the conversion between measured signals (voltage or counts) in W/(m^2 sr) or to Photons/(m^3 s) according to equations (2) and (4). An absolute calibrated system provides calibrated spectra, which gives direct access to plasma parameters. Thus, the effort is compensated by an increase in information. For the intensity calibration light sources are required for which the spectral radiance is known. One of the most critical points in the calibration procedure is the imaging of the light source to the spectroscopic system. Here one must be very careful to conserve the solid angle which is often adjusted by using apertures. Calibration standards in the visible spectral range, from 350 nm up to 900 nm, are tungsten ribbon lamps, providing black body radiation (grey emitter) and Ulbricht spheres (diffusive sources). For extensions to the uv range down to 200 nm, the continuum radiation of deuterium lamps is commonly used. Since such light sources must have high accuracy they are usually electrical stabilized but they alter in time. This means that their lifetime as calibration source is limited, which is less critical for relative calibration. Typical curves of a calibration procedure are shown in figure 7. The upper part is the spectral radiance of an Ulbricht sphere (provided by an enclosed data sheet) which is typically used for the calibration of a spectroscopic system with fibre optics. The spectrum in the middle gives the measured intensity in units depending on the detector (e.g. CCD detector, counts per second). The recorded spectrum is already normalized to the exposure time. Dividing the spectral radiance curve by the recorded spectrum the conversion factor is obtained representing the spectral sensitivity of the system. As already mentioned, absolutely calibrated spectral systems are the most powerful tool in plasma diagnostics. Thus, the following sections discuss the analysis methods based on absolutely calibrated spectra. Nevertheless, some basic principles can be
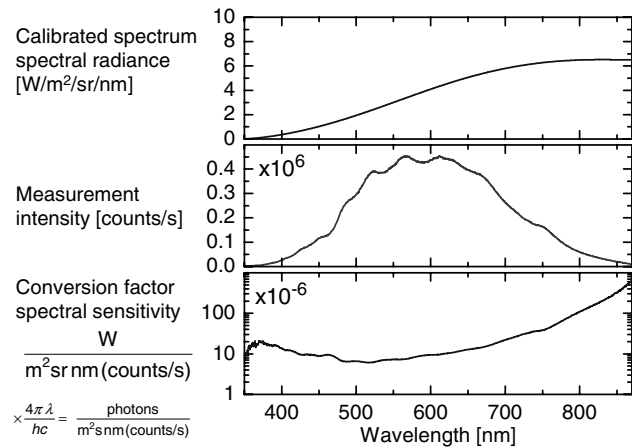

Figure 7. Example for the three steps needed to obtain a calibration curve.

applied even if only relatively calibrated systems or systems without calibration are available.

3. Population models

According to equation (4), the absolute intensity of a transition is directly correlated to the population density in the excited state, the upper level. The population density of excited states is described by a Boltzmann distribution provided that the levels are in thermal equilibrium among each other. Since low temperature plasmas are non-equilibrium plasmas, which means they are far from (local) thermal equilibrium, the population density does not necessarily follow a Boltzmann distribution. As a consequence, the population in an excited state depends not only on the electron temperature but on a variety of plasma parameters: temperature and density of the electrons and the heavy particles, radiation field, etc. The dominant parameters are determined by the dominant plasma processes. Thus, population models are required which consider populating and depopulating processes for each individual level of a particle. An excellent overview of this topic is given in [5]. It is obvious that for molecules where vibrational and rotational levels exist, the number of processes is incalculable and has to be reduced in some way.

3.1. Populating and depopulating processes

The electron impact excitation process is one of the most important processes. It increases the population of the upper level and decreases the population of the lower level. In turn electron impact de-excitation depopulates the upper level and populates the lower level. In a similar way, this principle applies to absorption and spontaneous emission for optically allowed transitions. Other population processes which couple with the particle in the next ionization stage are radiative or three-body recombination of the ion and the de-excitation by ionization. The different types of processes and a detailed explanation with examples are given in [4, 5, 7, 24].

Each process is described by its probability. In the case of spontaneous emission the probability is called the Einstein transition probability A_{ik}, where i labels the upper level and k the lower level. Collisional processes are generally described by cross sections or rate coefficients. The latter
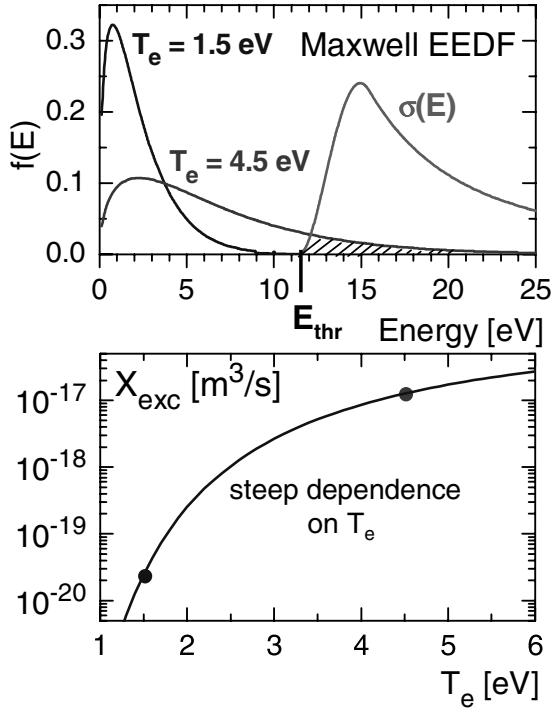
Figure 8. Convolution of a cross section with Maxwellian EEDFs ($T_e = 1.5$ eV and 4.5 eV) resulting in the excitation rate coefficient.

can be obtained from the convolution of the cross section with the corresponding energy distribution function of the impact particle. For an electron impact process the electron energy distribution is used, often described by a Maxwell distribution function. However, it should be kept in mind that this assumption is often not justified in low temperature plasmas, as briefly discussed in section 4.3. The upper part of figure 8 shows Maxwellian electron energy distribution functions (EEDF) $f(E)$ for two electron temperatures, $T_e = 1.5$ eV and $T_e = 4.5$ eV, and a typical cross section $\sigma(E)$ (in arbitrary units) for an electron impact excitation process. The dashed area starting with the threshold energy of the excitation process (E_{thr}) indicates the part of the electrons which contributes to the rate coefficient. The lower part of figure 8 shows the corresponding excitation rate coefficient $X_{\text{exc}}(T_e)$:

$$X_{\text{exc}}(T_e) = \int_{E_{\text{thr}}}^{\infty} \sigma(E)(2/m_e)^{1/2} \sqrt{E}\, f(E)\, \mathrm{d}E$$

with

$$\int_0^{\infty} f(E)\, \mathrm{d}E = 1. \qquad (6)$$

It is obvious that the rate coefficient $X_{\text{exc}}(T_e)$ shows a steep dependence on T_e, in particular, at low electron temperatures, i.e. $T_e < E_{\text{thr}}$. Since the part of the cross section with energies close to the threshold energy contributes most to the convolution, the accuracy of the rate coefficient depends strongly on the quality of the cross section in this energy region.

3.2. Corona model

A simple approach to population densities in non-equilibrium plasmas is presented by the so-called corona model. The corona equilibrium is deduced from the solar corona where

electron density is low ($\approx 10^{12}$ m^{-3}), electron temperature is high (≈ 100 eV) and where the radiation density is negligible. Due to the low electron density the probability of electron impact de-excitation processes is much lower than de-excitation by spontaneous emission and can be neglected. The electron temperature guarantees that the plasma is an ionizing plasma, i.e. recombination and thus populating processes from the next ionization stage do not play a role. Due to the insignificant radiation field, absorption is not important and excitation takes place only by electron impact collisions. Since these conditions are often fulfilled in low pressure, low temperature plasmas the usage of the corona model is a common method to deduce population (and ionization) equilibrium. However, the applicability has to be checked carefully in the individual case. These plasmas are characterized by a low degree of ionization. Each particle species (electrons, ions and neutrals) is characterized by its own temperature (under the assumption that a Maxwellian EEDF can be applied) and a gradual decrease is obtained: $T_e > T_i \geqslant T_n$.

The corona model assumes that upward transitions are only due to electron collisions while downward transitions occur only by radiative decay. Thus, in the simplest case, the population of an excited state p is balanced by electron impact excitation from the ground state $q = 1$ and decay by spontaneous emission (optically allowed transitions to level k):

$$n_1\, n_e\, X_{1p}^{\text{exc}}(T_e) = n(p) \sum_k A_{pk}\,. \qquad (7)$$

As discussed above, inverse processes, such as electron impact de-excitation and self-absorption, are not of relevance. As a result the population density is far below a population density according the Boltzmann distribution and population densities of excited levels are orders of magnitude lower than the population of the ground state. In this case, the ground state density n_1 can be replaced by the overall particle density n_n.

The corona equation can be extended easily by further processes, for example, excitation out of metastable states or cascading from higher excited states. For excited states without an optically allowed transition, i.e. metastable states, the losses are often determined by diffusion. This can be characterized by confinement times where the reciprocal value replaces the transition probability in equation (7). However, the selection of processes being important for the population equilibrium is often very unclear in the individual case.

3.3. Collisional radiative model

A more general approach to population densities is to set up rate equations for each state of the particle together with the coupling to other particles, e.g. the next ionization stage. Since such a model balances the collisional and radiative processes the model is called a collisional radiative (CR) model. The time development of the population density of state p in a CR-model is given by:

$$\frac{\mathrm{d}\, n(p)}{\mathrm{d}\, t} = \sum_{k<p} n(k)\, n_e\, X_{kp}^{\text{exc}}$$
$$- n(p) \left[n_e \left(\sum_{k<p} X_{pk}^{\text{de-exc}} + \sum_{k>p} X_{pk}^{\text{exc}} + S_p \right) + \sum_{k<p} A_{pk} \right]$$

$$+n(k) \sum_{k>p} \left(n_e \, X_{kp}^{\text{de}-\text{exc}} + A_{kp} \right)$$

$$+n_i \, n_e \left(n_e \, \alpha_p + \beta_p \right) . \qquad (8)$$

The first term describes the electron impact excitation from energetically lower lying levels, $k < p$. Loss processes are electron impact de-excitation into energetically lower lying levels, $k < p$, electron impact excitation of energetically higher lying levels $k > p$, electron impact ionization (rate coefficient ($S(p)$)), and spontaneous emission. Next, electron impact processes and spontaneous emission from energetically higher lying levels $k > p$ is taken into account. The last two expressions describe population by three-body recombination and radiative recombination respectively. In addition, opacity, which means self-absorption of emission lines, may be important. A convenient method is to use the population escape factors ([25, 26]) which reduce the corresponding transition probabilities in equation (8).

In the quasi-stationary treatment the time derivative is neglected $(\mathrm{d}\, n(p)/\mathrm{d}\, t = 0)$. However, transport effects may be of importance for the ground state and metastable states. This has to be taken into account by introducing diffusion or confinement times. According to the quasi-steady-state solution the set of coupled differential equations (8) is transformed into a set of coupled linear equations which depends on the ground state density and ion density. These equations are readily solved in the form

$$n(p) = R_n(p) \, n_n \, n_e + R_i(p) \, n_i \, n_e . \qquad (9)$$

$R_n(p)$ and $R_i(p)$ are the so-called collisional–radiative coupling coefficients describing ground state and ionic population processes, respectively. In ionizing plasmas, the coupling to the ground state is of relevance, whereas in recombing plasmas the coupling to the ionic state dominates.

In contrast to the corona model, the population of an excited state in the CR model depends on more parameters than on the electron temperature only. The population coefficients depend on electron temperature and electron density. Further parameters can be temperature and density of other species such as neutrals. In general, the CR model closes the gap between the corona and Boltzmann equilibrium. Figure 9 shows an example for population densities (normalized to the ground state) of the first electronically excited states of atomic hydrogen at $T_e = 3\,\text{eV}$ (ionizing plasma). The different regimes are indicated as well.

Since CR models depend strongly on the underlying data, it is obvious that the quality of results from CR models rely on the existence and quality of the cross sections (or rate coefficients). CR models are well established for atomic hydrogen, helium and argon which are elements with clear atomic structure. For molecules, CR models are scarce due to the manifold of energy levels to be considered and to the lack of data. Preliminary models for molecular hydrogen and molecular nitrogen are now available. The complexity of such models requires comparisons with experimental results in a wide parameter range, i.e. validations of models by experimental results.

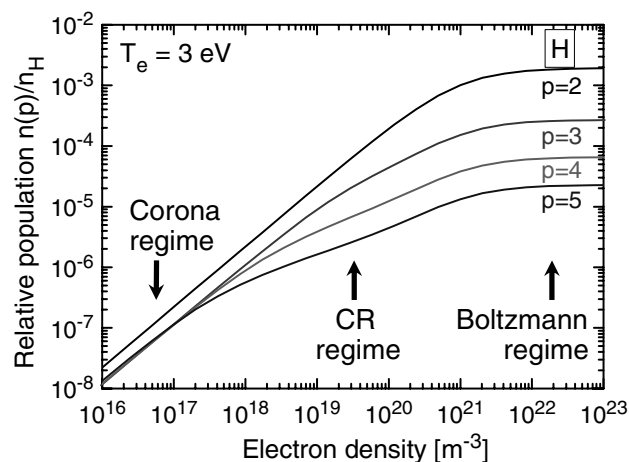The correlation between measured line emission and results from CR calculations are given by combining

Figure 9. Results obtained from a CR model for atomic hydrogen.

equations (4) and (9):

$$\frac{I_{pk}}{n_n \, n_e} = \frac{n(p)}{n_n \, n_e} A_{pk} = \left(R_n(p) + R_i(p) \, n_i / n_n \right) A_{pk} = X_{pk}^{\text{eff}} . $$

$$(10)$$

X_{pk}^{eff} is the effective emission rate coefficient, depending not only on T_e but also on other plasma parameters such as n_e, T_n, n_n, etc. .

4. Diagnostic methods

In this section the most common diagnostic methods of emission spectroscopy, suitable for direct application to low temperature plasmas, are described. More details about specific topics can be found in the literature. Some basic physics results for plasma spectroscopy and modelling are introduced in [27], whereas [28] focuses on atomic and molecular emission spectroscopy of hydrogen and deuterium plasmas. Application for industrial low pressure plasmas is given in [29] and [30] discusses applications to the cold plasma edge of fusion experiments. In general, it should always be kept in mind that plasma spectroscopy provides only line-of-sight averaged parameters.

In principle the methods can be applied to both ionizing and recombining plasmas; however, this discussion is carried out using ionizing plasmas as an example. An absolutely calibrated system is assumed but some of the basic principles can also be applied for a relatively calibrated system. The underlying formula for quantitative analysis of line radiation is given by rearranging equation (10):

$$I_{pk} = n_n \, n_e \, X_{pk}^{\text{eff}}(T_e, n_e, ...) . \qquad (11)$$

The emission rate coefficient is taken either from the CR model or from the corona model which is the convolution of the direct cross section with the EEDF.

4.1. Identification of particles

One of the easiest tasks of emission spectroscopy is the identification of particle species (atoms, ions, molecules) in the plasma, provided that the particles emit radiation. Since the line position, i.e. the wavelength is a fingerprint of an

element, it is sufficient to use a wavelength calibrated (survey) spectrometer with simple fibre optics in combination with wavelength tables for atoms, ions and molecules. Line identification can get complicated due to the presence of lines from higher orders of diffraction; however these can easily be suppressed by using suitable edge filters. In the case of diatomic molecules vibrational bands coupled with an electronic transition are observed and the position of the band head together with the shading is used for identification (see N_2 spectrum in figure 5). An exception is molecular hydrogen (and deuterium) which has a multi-line spectrum due to its small mass. Identification of molecular radiation is best done with the book by Pearse and Gaydon [31]. Precise wavelengths and transition probabilities for atoms and ions can be found in the NIST database [23]. It should be kept in mind that the Doppler effect, which is caused by the particle velocity, results in a shift of the central wavelength. However, this shift is usually very small and its detection needs a spectroscopic system with high spectral resolution. On the other hand, the measurement of the Doppler shift provides a tool to determine the velocity of the emitting particle.

Besides the filling gases, ionized particles and dissociation products, i.e. radicals can be identified. In addition, impurities are detected immediately: water (OH, and O radiation), air (N_2 and NO radiation) or particles released from a surface by sputtering.

4.2. Line broadening and gas temperature

Precise measurements of line profiles are a valuable tool in plasma diagnostics with which a manifold of parameters can be obtained. On the experimental side this requires a spectroscopic system with high spectral resolution as provided by Echelle spectrometers or Fabry–Perot set-ups. For evaluating data the underlying line broadening mechanism is of importance. Besides the natural line broadening, Doppler broadening, pressure broadening, broadening by electrical fields (Stark broadening) and magnetic fields (Zeeman effect) may contribute to the line shape. These are in addition to broadening by the apparatus itself. The Doppler broadening offers a tool to determine the gas temperature (see below), whereas electrical fields, i.e. electron density can be determined from the Stark broadening and magnetic field strengths are obtained from the Zeeman broadening. The latter two mechanisms are of importance in dense plasmas (high electron density) and in strong magnetic fields, respectively. Details of line broadening mechanisms and their applications to plasma diagnostics can be found in, e.g., [3, 32, 33].

Under the assumption that Doppler broadening is the dominant line broadening mechanism, the gas temperature (heavy particle temperature) can be obtained from precise measurements of the line profile, in particular the line width. However, in the analysis of a measured peak width $\Delta\lambda_{FWHM}$, the apparatus profile $\Delta\lambda_A$, has to be taken into account:

$$\Delta\lambda_{FWHM} = \sqrt{(\Delta\lambda_D)^2 + (\Delta\lambda_A)^2} , \qquad (12)$$

assuming the same line profile for both mechanisms, Gaussian in this case. Thus, the maximum apparatus profile as an upper limit can be estimated which allows the measurement of the
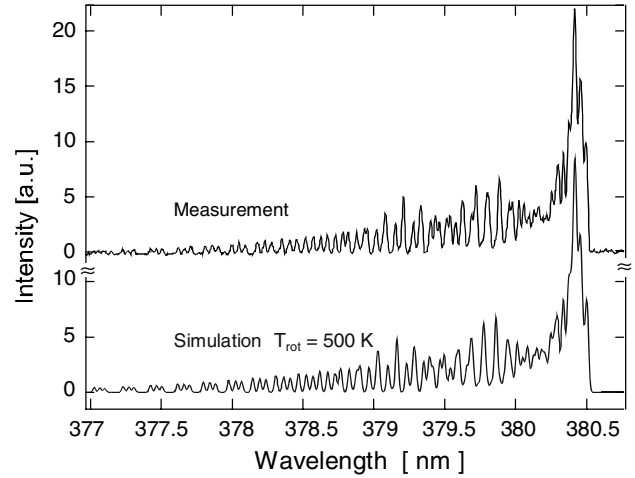
Figure 10. Gas temperature obtained from the fit of the computer simulation to the measurement of a vibrational band of N_2.

gas temperature with sufficient accuracy. Since the Doppler broadening

$$\Delta\lambda_D = 2\sqrt{\ln 2}\,\lambda_0\sqrt{\frac{2kT_{gas}}{mc^2}} \qquad (13)$$

is stronger for light elements and high central wavelengths, the Balmer line H_α is a favourite for this diagnostic purpose.

An alternative method is the analysis of rotational lines of a vibrational band of a diatomic molecule. Here, vibrational bands of molecular nitrogen or its ion are commonly used. If nitrogen is not part of the gas mixture, it is sufficient to add (just for diagnostic purposes) a small percentage of nitrogen to the discharge. Since the energy distance between rotational levels in one vibrational state is usually very small, typically a tenth of an electronvolt, the rotational population can be characterized by a rotational temperature T_{rot} (Boltzmann population). $T_{rot}(v')$ is obtained either from a Boltzmann plot or from a comparison of measured vibrational bands ($v'-v''$) with simulations of spectra based on molecular constants. This is shown in figure 10 for the $v' = 0 - v'' = 2$ band of the electronic transition $C\,^3\Pi_u - B\,^3\Pi_g$ of N_2. The shape of the vibrational band is sensitive to T_{rot} which is the only fit parameter in the simulation. Under the assumption that the rotational quantum number is conserved by the electron impact excitation process (Franck–Condon principle), T_{rot} in the excited state represents T_{rot} in the ground state. If in addition the rotational levels of the ground state are populated by heavy particle collisions, this temperature reflects the gas temperature. The method works well for this particular band of nitrogen; however one has to be careful with the analysis if the argon is also a part of the gas mixture. Due to the similar excitation energy of Ar and N_2 excitation transfer from the metastable states of argon contributes to the $C\,^3\Pi_u$ population of nitrogen resulting in higher rotational temperatures that no longer reflect the true gas temperature. In this case, the vibrational bands of N_2^+ ($B\,^2\Sigma_u^+ - X\,^2\Sigma_g^+$ transition, first negative system) should be used for the analysis.

4.3. Electron energy distribution function and electron temperature

The electron temperature is one of the key parameters in low temperature plasmas and in the analysis of line emission. However, it should be kept in mind, that T_e is defined only in the case of a Maxwellian energy distribution function, which is not generally valid. Common methods to determine the EEDF are Langmuir probe measurements or calculations based on the solution of the Boltzmann equation. Emission spectroscopy can be used to get information about deviations of an EEDF from the Maxwell case. According to equations (4) and (6) the part of the EEDF above the threshold energy of the excitation process contributes to the line radiation. Thus, evaluation of lines with different energy thresholds represents an energy scan. The main task is to find suitable diagnostic gases and emission lines where the corresponding cross sections are very reliable in the energy region close to the threshold energy. The diagnostic method itself is discussed in [34] using lines of rare gases, e.g. helium lines with $E_{\mathrm{thr}} \approx 23$ eV and argon lines with $E_{\mathrm{thr}} \approx 13$ eV. Extensions to the low energy range are introduced in [35] by analysing the vibrational bands of molecular nitrogen. In order to apply the method, a spectroscopic system with a moderate spectral resolution, wavelength calibration and relative intensity calibration is required.

The choice of the diagnostic method for the determination of electron temperature depends on the type of the spectroscopic system and on the degree of information on the other plasma parameters, in particular, electron density, which can be measured by Langmuir probes or microwave interferometry.

The line ratio method is based on the same principle as the determination of the EEDF. According to equation (11), the direct dependence on electron density cancels in any line ratio:

$$\frac{I_{pk}^1}{I_{lm}^2} = \frac{n_1}{n_2} \frac{X_{pk}^{\mathrm{eff}}(T_e, n_e, ...)}{X_{lm}^{\mathrm{eff}}(T_e, n_e, ...)} \ . \tag{14}$$

The dependence of the line ratio on T_e is derived by either using emission lines from different gases with different energy threshold or from lines of a single gas which have different shapes of the cross section. The latter is achieved by using cross sections which correspond to excitation of an optically allowed transition and an optically forbidden transition. The usage of emission lines from different gases requires knowledge of the particle densities whereas the particle densities cancel in the line ratio of emission lines from a single gas. It is also essential that the excitation from the ground state is the dominant population mechanism so that the dependence of the effective rate coefficient on electron density vanishes. Prominent examples are the line ratio of helium to argon or the line ratio of helium lines (triplet to singlet system). The upper part of figure 11 shows the ratio of emission rate coefficients corresponding to the line ratio of the He line at 728 nm to the Ar line at 750 nm. It is obvious that the line ratio is particularly sensitive to the electron temperature at low T_e. The weak radiation of the He line in comparison to the Ar line (a factor of 100 less at $T_e = 3$ eV for equivalent particle densities) can be compensated for by adjusting the density ratio accordingly.
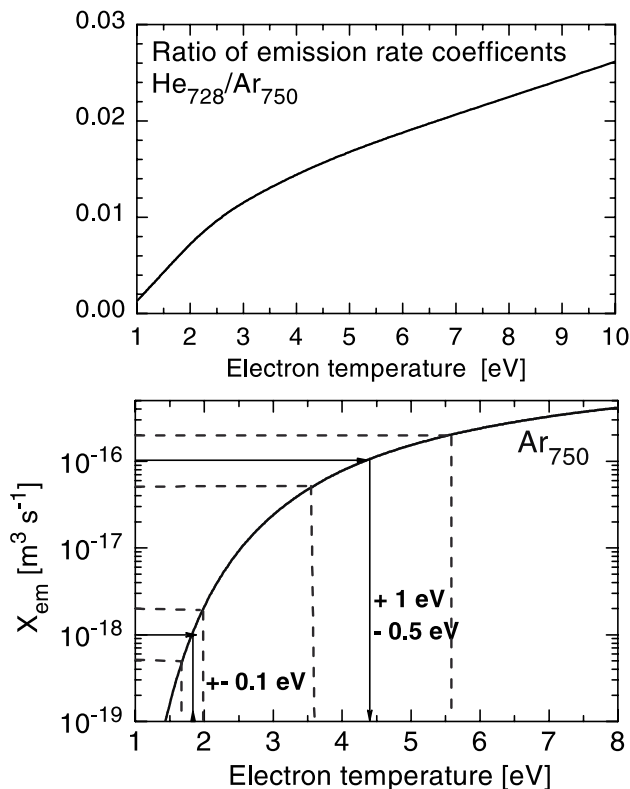

Figure 11. Determination of electron temperature using an appropriate ratio of emission rate coefficients or using the emission rate coefficient directly.

The second and more precise method for determining the electron temperature is the analysis of the absolute line radiation. To do this requires an absolutely calibrated spectroscopic system and knowledge of the electron density. If one uses a rare gas, the particle density can be calculated by the general gas law, provided the gas temperature is known. In this case the remaining unknown in equation (11) is the rate coefficient which is strongly dependent on electron temperature. In the lower part of figure 11 is shown the emission rate coefficient of the Ar line at 750 nm. The steep dependence of the rate coefficient on electron temperature results in a high accuracy for the electron temperature at low T_e as indicated in figure 11 by the arrows and dashed lines. An experimental error of a factor of two is assumed. For diagnostic purposes it is sufficient to only add a small amount of argon to the discharge. This can be done only when the key parameters of the discharge will not change by the admixture.

4.4. Particle densities

Determination of particle densities is done in a manner similar to that used for the electron temperature. Again one has to choose using either the line ratio method or the analysis of absolute intensities; which method one chooses depends on the spectroscopic system available. The line ratio method, also known as actinometry, requires the precise knowledge of the electron temperature or a ratio of emission rate coefficients with only a weak dependence on T_e. The latter condition is usually fulfilled if diagnostic lines are used with similar excitation thresholds and similar shape of cross sections.

A popular example of actinometry is with atomic hydrogen, using an argon admixture, both having a threshold energy of $E_{\text{thr}} \approx 13$ eV for the first excited states. The ratio of the emission rate coefficients for the Balmer emission line H_γ and the argon line at 750 nm is almost constant for $T_e > 2.5$ eV. Since the argon density is usually known from the percentage of admixture, the atomic hydrogen density can be derived from equation (14).

The analysis of absolute line radiation can be applied if electron density and electron temperature are known. This method has the advantage that an additional diagnostic gas is not required. It must be ensured that the ground state excitation channel is the dominant one to use this method; however, additional excitation processes can be important also. A good example of the effect of other excitation processes is given by the case of Balmer line radiation excitation from molecular hydrogen. This dissociative excitation process might be of relevance, in particular, for plasmas with low degree of dissociation. In addition, self-absorption of resonance lines, the so-called opacity, may contribute to line emission. In the case of atomic hydrogen, lines of the Lyman series become optically thick and thus enhance the population of excited states in comparison with the optically thin case. Details of both mechanisms, dissociative excitation and opacity, are discussed for Balmer line radiation in [26].

4.5. Insight in plasma processes

The light emitted is sensitive to changes in plasma parameters such as particle temperatures and densities, formation of radicals, impurities, rotational and vibrational population. Thus spectra can be used as a tool to gain insights into plasma processes. The majority of the information can be obtained by using an absolutely calibrated system with moderate spectral resolution. Measurements of a variety of transitions of one particle species can be used to check the analysis for consistency. In combination with a CR model such measurements provide information about the importance of opacity, cascading, quenching, population and diffusion time of metastable states. The most reasonable procedure is to measure as many population densities of excited states as possible and compare the experimental results with predictions of the CR model.

The radiation of radicals that are formed by dissociation of parent molecules is a very valuable indicator for dissociation processes. For example, in a plasma containing methane the methane dissociates by electron impact in methane radicals such as CH_3, CH_2, CH and C. These radicals contribute to the formation of higher hydrocarbons by heavy particle collisions. In general, the whole process chain can be described by dissociation models. Radiation of diatomic radicals, such as CH and C_2 is readily identified in the spectrum. The rotational structure of vibrational bands can be used to obtain the rotational population characterized by a rotational temperature. As discussed in section 4.2 a rotational temperature may correspond to the gas temperature. However, for dissociation products, the parent molecules can contribute to the rotational population of the radical by the dissociative excitation process. Typically, deviations from the true gas temperature are observed resulting in a
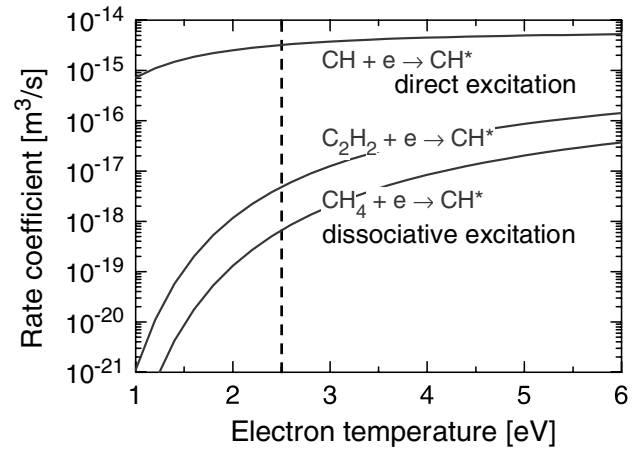

Figure 12. Three channels contributing to the emission of the CH radical ($A\,^2\Delta - X\,^2\Pi$ transition, $v' = v'' = 0 - 2$): direct excitation and dissociative excitation from CH_4 and C_2H_2.

two temperature distribution. Thus, the importance of the dissociative excitation mechanism can be derived from the rotational population.

The analysis of absolute intensities offers a method to quantify the contribution of the excitation channels to the emission spectrum. For example, the radiation of the CH radical can originate from the direct excitation (CH + e $\rightarrow$ CH*; the asterisk denotes an excited state) and the dissociative excitation from the parent molecule CH_4 and from higher hydrocarbons: CH_4 + e $\rightarrow$ CH* + 3H and C_2H_y + e $\rightarrow$ CH* + CH_{y-1}. The contribution from these three processes to the overall radiation of the CH molecule depends strongly on the three densities (CH, CH_4 and C_2H_y) and on the electron temperature. Figure 12 shows the emission rate coefficients of CH $A\,^2\Delta - X\,^2\Pi$ transition, $v' = v'' = 0$–2) for these three processes. At $T_e = 2.5$ eV the dissociative excitation channels are three to four orders below the direct excitation channel; however, the dissociative excitation by CH_4 might be the dominant population path due to the much higher density of this particle species in a methane plasma. Systematic investigations can lead to a simplified diagnostic method, such as the monitoring of a particle density ratio (C_2H_y/CH_4) by the intensity ratio of molecular bands (C_2/CH) [29].

5. Conclusion

Plasma spectroscopy which focuses on atomic and molecular emission spectroscopy of low temperature plasmas is a powerful diagnostic tool. The most common spectroscopic systems and analysis methods have been described with emphasis on the determination of the various plasma parameters. Examples are presented, ready for direct application by the reader. In general, the great advantages of plasma spectroscopy are the simple experimental set-up and that it provides a non-invasive and *in situ* diagnostic method. Spectra are recorded easily but the interpretation of those spectra can be a complex task. However this is compensated for by the variety of valuable results one can achieve. Explore your plasma with plasma spectroscopy!

References

[1] Griem H R 1964 *Plasma Spectroscopy* (New York: McGraw-Hill)

[2] Lochte-Holtgreven W 1968 *Plasma Diagnostics* (Amsterdam: North-Holland)

[3] Griem H R 1997 *Principles of Plasma Spectroscopy* (Cambridge: Cambridge University Press)

[4] Thorne A, Litzen U and Johansson S 1999 *Spectrophysics: Principles and Applications* (Berlin: Springer)

[5] Fujimoto T 2004 *Plasma Spectroscopy* (Oxford: Clarendon)

[6] Chen F F and Chang J P 2003 *Lecture Notes on Principles of Plasma Processing* (New York: Kluwer)

[7] Hippler R, Pfau S, Schmidt M and Schoenbach K H eds 2001 *Low Temperature Plasma Physics* (Berlin: Wiley)

[8] Huddlestone R H and Leonard S L 1965 *Plasma Diagnostic Techniques* (New York: Academic)

[9] Hutchinson I H 1987 *Principles of Plasma Diagnostics* (Cambridge: Cambridge University Press)

[10] Auciello O and Flamm D C 1989 *Plasma Diagnostics Vol. 1* (San Diego: Academic)

[11] Dean J R 1997 *Atomic Absorption and Plasma Spectroscopy* (Chichester: Wiley)

[12] Dean J R 2005 *Practical Inductively Coupled Plasma Spectroscopy* (Chichester: Wiley)

[13] Payling R, Jones D G and Bengtson A 1997 *Glow Discharge Optical Emission Spectrometry* (New York: Wiley)

[14] Nelis T and Payling R 2004 *Glow Discharge Optical Emission Spectroscopy: A Practical Guide* (Cambridge: Royal Society of Chemistry)

[15] Buuron A J M, Otorbaev D K, van de Sanden M C M and Schram D C 1994 *Rev. Sci. Instrum.* **66** 968–74

[16] Booth J P, Cunge G, Neuilly F and Sadeghi N 1998 *Plasma Sources Sci. Technol.* **7** 423–30

[17] Herzberg G 1944 *Atomic Spectra and Atomic Structure* (New York: Dover)

[18] Sobelman I I 1979 *Atomic Spectra and Radiative Transitions* (Berlin: Springer)

[19] Cowan R D 1981 *The Theory of Atomic Structure and Spectra* (Berkeley, CA: University of California Press)

[20] Erkoc S and Uzer T 1996 *Lecture Notes on Atomic and Molecular Physics* (Singapore: World Scientific)

[21] Herzberg G 1989 *Molecular Spectra and Molecular Structure I. Spectra of Diatomic Molecules* (Malabar, FL: Krieger)

[22] Bernath P F 1995 *Spectra of Atoms and Molecules* (Oxford: Oxford University Press)

[23] NIST database http://physics.nist.gov/PhysRefData/

[24] Chapman B 1980 *Glow Discharge Processes* (New York: Wiley) Chapter 2

[25] Irons F E 1979 *J. Quantum Spectrosc. Radiat. Transfer* **22** 1–20

[26] Behringer K and Fantz U 2000 *New. J. Phys.* **2** 23.1–23.19

[27] Behringer K and Fantz U 1999 *Contrib. Plasma Phys.* **39** 411–25

[28] Fantz U 2002 Atomic and molecular emission spectroscopy in low temperature plasmas containing hydrogen and deuterium *IPP Report* IPP 10/21

[29] Fantz U 2004 *Contrib. Plasma Phys.* **44** 508–15

[30] Fantz U 2005 Molecular diagnostics of fusion and laboratory plasmas *Atomic and Molecular Data and Their Applications (AIP Conf. Proc. Series vol 771)* ed T Kato *et al* (New York: Springer-Verlag) p 23–32

[31] Pearse R W B and Gaydon A G 1950 *The Identification of Molecular Spectra* (New York: Wiley)

[32] Griem H R 1974 *Spectral Line Broadening by Plasmas* (New York: Academic)

[33] Sobelman I I, Vainshtein L A and Yukov E A 1998 *Excitation of Atoms and Broadening of Spectral Lines* (Berlin: Springer)

[34] Behringer K and Fantz U 1994 *J. Phys. D: Appl. Phys.* **27** 2128–35

[35] Vinogradov I P 1999 *Plasma Sources Sci. Technol.* **8** 299–312